

Pixel Local Supports FDR

ATLAS Project Document No:

ATL-IP-ER-0004

Institute Document No.

Created: **7/6/2000**

Page: **1 of 28**

Modified:

Rev. No.: *1*

ATLAS PIXEL LOCAL SUPPORTS (DISK SECTOR)

DESIGN STATUS AND PLAN

This document summarizes the design status and tests of prototypes of the ATLAS Pixel System Local Supports for the disk sectors. A summary of a plan of work leading up to the Production Readiness Review is also given.

Prepared by:

E. Anderssen, M. Gilchriese, F. Goozen, G. Hayman, F. McCormack, W. K. Miller, W. O. Miller, J. Taylor, T. Weber, J. Wirth

Checked by:

Approved by:

Distribution List

History of Changes

<i>Rev. No.</i>	<i>Date</i>	<i>Pages</i>	<i>Description of changes</i>

Table of Contents

1	INTRODUCTION	4
2	DISK SECTORS	4
2.1	Design and Prototype History and Status Summary.....	4
2.1.1	Overview	4
2.1.2	Carbon-tube Design	4
2.1.3	Sealed-tube Design.....	5
2.1.4	Aluminum-tube Design	7
2.2	Thermal Performance.....	8
2.2.1	Introduction	8
2.2.2	Test Samples and Single Sectors.....	9
2.3	Stability Performance	15
2.3.1	Introduction	15
2.3.2	Test Samples and Single Sectors.....	16
2.4	Prototype Disk	20
2.5	Material.....	22
2.6	Miscellaneous.....	23
2.7	Interfaces.....	24
2.7.1	Mounting to the Disk Support Ring	24
2.7.2	Coolant Connections	24
2.7.3	Module Attachment.....	24
2.7.4	Electrical	25
2.8	Summary of Status and Critical Outstanding Issues	25
3	WORK PLAN SUMMARY	27
3.1	Introduction	27
3.2	Sealed-tube Plan	27
3.3	Aluminium-tube Plan.....	27

1 Introduction

This note summarizes the design status and measurements on prototypes of the ATLAS Pixel Local Supports - the Disk Sectors. A proposed plan of work leading up to the Production Readiness Review (PRR) is also provided. This note assumes familiarity with the ATLAS Pixel System¹ and the corresponding local-support requirements.²

2 Disk Sectors

2.1 Design and Prototype History and Status Summary

2.1.1 Overview

Three different types of disk sectors have been designed and prototypes fabricated. Tests have been performed on these prototypes to determine if the designs meet the requirements. The design concept for each of these prototypes is summarized here. A more detailed description of the fabrication process for two of the designs - those based on aluminum cooling tubes and sealed carbon-carbon tubes - is available.³ All disk sector designs share the common feature of having carbon-carbon faceplates. The carbon-carbon faceplates have high in-plane thermal conductivity, adequate transverse thermal conductivity and high stiffness. Pixel modules are mounted on both sides of the sector. Coolant is contained in a tube between the faceplates that is arranged to meet the thermal requirements with the minimum material (for each design). The three different designs differ in the composition of the cooling tube, how the tube is attached to the faceplates and how structural stiffness is maintained for the finished sector.

A complete set of measurements does not yet exist to demonstrate that all requirements, including the interface requirements,⁴ can be met. An enumeration of outstanding issues and a plan to address them are included in this note.

2.1.2 Carbon-tube Design

The carbon-tube design was developed by Energy Sciences Laboratory, Inc (ESLI)⁵ under a direct contract from the US Department of Energy. The coolant tube is a glassy carbon tube that can be formed as shown in Figure 1. The tube is mechanically and thermally connected to the faceplates by using high-thermal-conductivity fibers that are "flocked" onto the carbon tube and machined flat, using a proprietary process from ESLI. The concept is illustrated in Figure 2. The resulting structure is then thermally and otherwise processed to provide an all-carbon structure with good matching of the coefficients of thermal expansion among the various sub-components. In part, the short fibers connecting the tube to the faceplates take up thermally-induced strains.

ESLI developed a number of generations of these prototypes. Nine prototypes were manufactured to develop the technique. These prototypes have been used in three critical tests to assess the ability of disk sectors to meet the design requirements. One, evaporative cooling tests (with C_4F_{10}) were performed in four different orientations of the sector to determine if gravity affected the evaporative cooling concept using a cooling tube with multiple bends. No significant differences were observed. Two, a later generation of prototype was used with evaporative cooling (also with C_4F_{10}) to understand operating margins and compare with theoretical calculations. These tests are described later. Third, ESLI produced an additional twelve prototype sectors (of which two developed leaks during handling) that were mounted on a prototype disk support ring. Extensive stability measurements were performed on this complete disk at simulated operating conditions. These tests are also described later.

ESLI is not currently considered to be a viable alternative for production of the disk sectors. The reasons for not considering them include cost, reliability of the design under pressure fault conditions, reliability of the fabrication process and schedule.



Figure 1. Glassy carbon tube manufactured by ESLI.



Figure 2. Glassy carbon tube with fibers attached.

2.1.3 Sealed-tube Design

The tube in this design has been developed by HYTEC, Inc⁶ under direct contract from the US Department of Energy. The tube is a resin-sealed carbon-carbon (C-C) tube developed by HYTEC, Inc⁷ and illustrated in Figure 3. It is attached to the faceplates with a rigid epoxy (right inset of Figure 3) and there is no material other than the tube between the faceplates. There is a very good match of coefficients of thermal expansion between the carbon-carbon tube and the carbon-carbon faceplates.

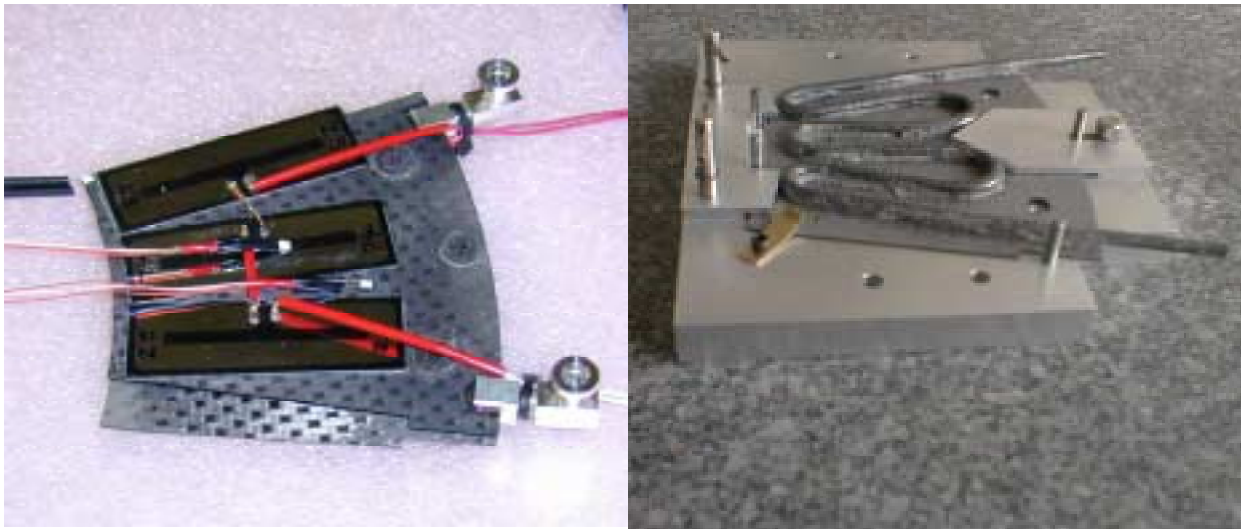


Figure 3. Left inset is photograph of a completed sector with a carbon-carbon sealed tube. The right inset illustrates the C-C tube bonded to the first faceplate, an initial step in the assembly process.

To date, 11 sectors have been built, 2 development sectors and 9 sectors as given in Table 1. Additional sectors are under fabrication to be completed by June 2000.

HYTEC is conducting a series of thermal, stability, and pressure tests on each sector. Table 1 lists the status of the sector testing. Thermal tests are performed at both room temperature and at -15°C inlet coolant temperature. The cold tests simulate the actual detector performance conditions and this condition is essential for conducting a stability test. Not all sectors are tested at -15°C . However, all sectors will be thermally tested with room temperature coolant. This test is conducted to validate thermal performance of each sector. Sector stability is recorded with a real-time holography system, PRISM, at HYTEC, for both cold and room temperature inlet conditions. Leak- and elevated-pressure tests are to be performed on all sectors. Elevated pressure testing on each sector comprises 10 cycles at 4 bar absolute and a 10 bar proof test. Exploratory high pressure tests were performed on units 3 and 4, cycling up to 150 times at 5 bar and single cycles to 10 bar. Mechanical strain data were recorded holographically throughout the pressure cycling. Sector #8 has been test at 8 bar absolute for one hour with no leakage.

Four sectors have been thermally tested with a methanol and water solution, as well as pure water. The methanol/water coolant is used to evaluate thermal performance at -15°C .

HYTEC is preparing to evaluate the thermal and stability performance of a dual sector arrangement with evaporative coolant, C_4F_{10} . This test is intended to demonstrate that no stability differences exist between a liquid and evaporative coolant system. It is believed that the stability, quantified by out-of-plane thermal strains, is entirely governed by the change from room temperature conditions to the sub-cooled operating state. In addition, one sector will be tested in June at CERN with the current baseline coolant, evaporative C_3F_8 .

Sector Unit #	Tube wall	Status	Weight ¹ -g
1	single	Development unit	n/a
2	single	Development unit	n/a
3	single	Thermal, stability, and pressure	21.02 ²
4	double	Thermal, stability, and pressure	23.84 ²
5	single	Pressure	21.63 ²
6	single	Thermal, stability, and pressure	19.17 ³
7	single	Pressure	17.5 ³
8 ⁴	single	Thermal, Pressure	17.93 ²
9	double	Pressure	21.25 ³
10	double	Pressure	21.01 ³
11	double	Pressure	20.32 ³
12	double	Under construction	
13	double	Under construction	
14	double	Under construction	
15	double	Under construction	
16	double	Under construction	

Table 1. List of HYTEC sector configurations and status.

The thermal structure depicted in Figure 3 utilizes high thermal conductivity facings, which are 0.5mm thick carbon-carbon, produced from a balanced 2D woven fabric of K321 fibers. The facings were lightly sanded to a 0.5mm thickness, after being carbonized and infiltrated with carbon (CVD). As carbonized and heat-treated, the facings are 0.7 mm thick.

¹ Weight without aluminum tube connections

² Carbon-carbon mounting bushings

³ PEEK mounting bushings

⁴ Tests with evaporative C_4F_{10} are in progress.

Initially, the tubes were configured to be a 3.2mm ID carbon tube with a wall thickness of 0.25 mm. The C-C tube wall is comprised of a matrix of carbonized phenolic resin, and a single layer of T300 woven carbon fibers. The tube was sealed with an overcoat of EPON815C resin. The mass⁵ for the sector with a 0.25 mm wall (unit #3) was 19.5 gm, with the C-C facings comprising 64% of the mass. The aluminum tube fittings are not included in the mass since they will be ultimately replaced.

In more recent sectors (Table 1), the coolant tube wall thickness was increased by a factor of two (unit #4). The wall thickness was increased primarily for added strength, but also to increase the surface area for heat conduction into the coolant fluid. The increased wall thickness was accomplished by using two layers of carbon fibers, as opposed to a single layer (unit #3). This change amounted to using two layers of the woven sock (braided fibers), an outer and inner layer. The combined woven sock layers were then impregnated with phenolic resin and carbonized. The same tooling was used in the processing the double and single fiber-layer tubes; hence, the thicker walled-tube developed a flatter appearance. Throughout the various processing steps, and subsequent tube sealing process, the robustness of the thicker-walled tube was quite evident. The tube weight increased from nominally 2.8 to 5.8gms. This change, if adopted, would increase the radiation length of the tube contribution in the active pixel detector area from 0.11 to 0.22%.

The sealed-tube design remains an option for the final production of disk sectors.

2.1.4 Aluminum-tube Design

The tube in this design is a bent, rectangular aluminum tube - see Figure 4. The thermal contact with the faceplates is provided by thermally conductive compound (CGL-7018 from AI Technologies) as shown in Figure 5. The tube is captured by densified, reticulated vitreous carbon (RVC) foam and a few carbon-carbon hard points that are rigidly bonded to the faceplates using a cyanate ester adhesive as also shown in Figure 5. The natural density of the RVC foam is doubled by manufacturers to 0.1 gm/cm³ by chemical vapor deposition (CVD) to increase the strength. These sectors have been designed and fabricated at Lawrence Berkeley National Laboratory.



Figure 4. Aluminum tube for disk sectors.



Figure 5. Anodized tube in foam showing construction.

Ten prototypes of this design have been fabricated (as of early June 2000) and additional prototypes are under fabrication. The basic parameters of these prototypes are summarized in Table 2. Test results for some of these sectors are reported below. Prototypes #1 and #2 were fabricated some years ago for disk layouts that are no longer relevant. Prototype #5 was poorly made and rebuilt to become prototype #6.

⁵ This mass may be trimmed further by decreasing the facing thickness slightly.

NUMBER	FACING THICKNESS	FILL MATERIAL CARBON FOAM	FILL TO C-C ADHESIVE	AL-TUBE
3	0.50 mm	0.05 gm/cc	3M-9460	Round 3.6 mm ID 0.20 mm wall
4	0.30	0.10	Cyanate ester	Round/flattened 3.6 mm ID 0.20 mm wal
5	0.30	0.10	Cyanate ester	Rectangular ID 1.69x4.06 mm 0.20 mm wall
6	0.30	0.10	Cyanate ester	Rectangular ID 1.69x4.06 mm 0.20 mm wall
7 and 8	0.42±0.03	0.10	Cyanate ester	Rectangular ID 1.69x4.06 mm 0.29 mm wall
9 and 10	0.42±0.03	0.10	Cyanate ester	Rectangular ID 2.74x4.19 mm 0.29 mm wall

Table 2. Summary of aluminum-tube prototype sectors.

This design is the current baseline for the disk sectors and thus is an option for the final production.

2.2 Thermal Performance

2.2.1 Introduction

The essential thermal requirement is to maintain the pixel silicon sensor temperature below -6°C with a uniformity across the sector of ≤10°C under all conditions. The thermal performance of the sectors has been assessed by attaching dummy heat loads to the sectors to simulate the heat load introduced by the pixel electronics. This has been done by evaporating thin platinum on 0.300 mm silicon in a pattern that simulates the pixel electronics and sensor leakage current heat loads. These resistive heaters are attached to the sectors in a manner similar to that expected for actual pixel module attachment. Thus the actual heat loads are simulated as well as can be done in the absence of real pixel modules.

Thermal measurements are done by infrared (IR) thermography coupled with measurements at discrete points using RTDs or other devices. The IR measurements are normalized to the single point measurements. The overall absolute accuracy in the temperature scale is estimated to be ±1.5°C. Two different types of IR cameras have been used so far.

The thermal performance of the sectors depends on a number of factors. These include the coolant temperature, the coolant flow rate, the temperature differential between the coolant and the surface of the sector faceplates and the temperature differential between the faceplate and the simulated pixel module. The last item is an interface to the sector, and imposes requirements on the module attachment that are not directly addressed here.

The current baseline coolant system is evaporative C₃F₈. Thermal performance tests on disk sector prototypes have been done with water/alcohol mixes, liquid fluorinert (C₆F₁₄) and evaporative C₄F₁₀ but NO tests have been done on disk sectors with the baseline coolant. First tests with the baseline coolant are planned in June 2000. Our test results exhibit a good correlation between the thermal performance measured with different fluids, in particular the temperature differential between the local

coolant (or coolant pipe) and the surface of the sector faceplates. Thus we believe measurements made with coolants other than evaporative C_3F_8 are reliable indicators of thermal performance, but this will be verified.

2.2.2 Test Samples and Single Sectors

Thermal measurements have been done on prototypes of the disk sectors and smaller test pieces used for pre- and post-irradiation comparisons.⁸ These test pieces were constructed in a manner similar to the sectors and are about equal in size to one-third of a sector, with dummy heaters on both sides.

2.2.2.1 Aluminum-tube Thermal Tests

The measurement of thermal performance of an aluminum-tube sector is illustrated in Figure 6 and Figure 7. The IR measurements are cross-referenced to measurements using RTDs at a few points on the platinum-plated, silicon dummy heaters. Measurements without power are taken to determine a base state and then measurements are taken at different power levels and coolant conditions. The coolant used in this example was a water/methanol mixture. Figure 6 and Figure 7 also show reference surfaces (points 3 and 4) that are used to calibrate the measurements. The measurements on aluminum-tube prototypes #4, #6, #7 and #8 can be summarized briefly as follows:

- the temperature differential between the bulk coolant temperature and the surface of the silicon simulated heaters can be kept $\leq 12^\circ C$ at full power (50 W) in the worst locations for flow conditions that are believed to approximate those that would prevail in evaporative C_3F_8 cooling;
- the uniformity of temperature can be $\leq 7^\circ C$ under the same conditions; and
- these temperature differentials are linear in the power, for fixed coolant temperature and flow.

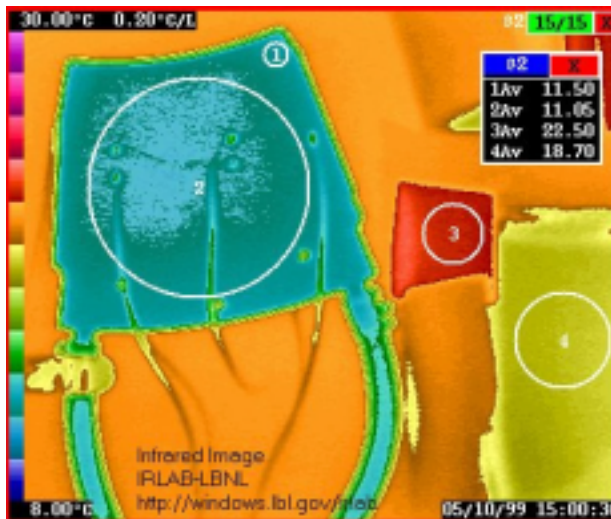


Figure 6. Infrared image of aluminum-tube prototype# 4 without power at 10 cc/sec flow of coolant.



Figure 7. Infrared image of aluminum-tube prototype #4 at 48W of power with 10 cc/sec flow of coolant.

The maximum temperature differential occurs near the edges of the sector, and additional design modifications (small movements of the aluminum tube) are being implemented to reduce further the maximum temperature differential. Tests of the sectors most recently fabricated indicate this has been successful - see Figure 8.

2.2.2.2 Sealed-tube Thermal Tests

Initial HYTEC sector thermal tests have been conducted in a dual-sector arrangement shown in Figure 9. RTD recordings of the temperature rise from power off to power on were made at six points on the thermal structure. The temperature increase is measured with respect to coolant inlet temperature, which remained constant at room temperature throughout the test.

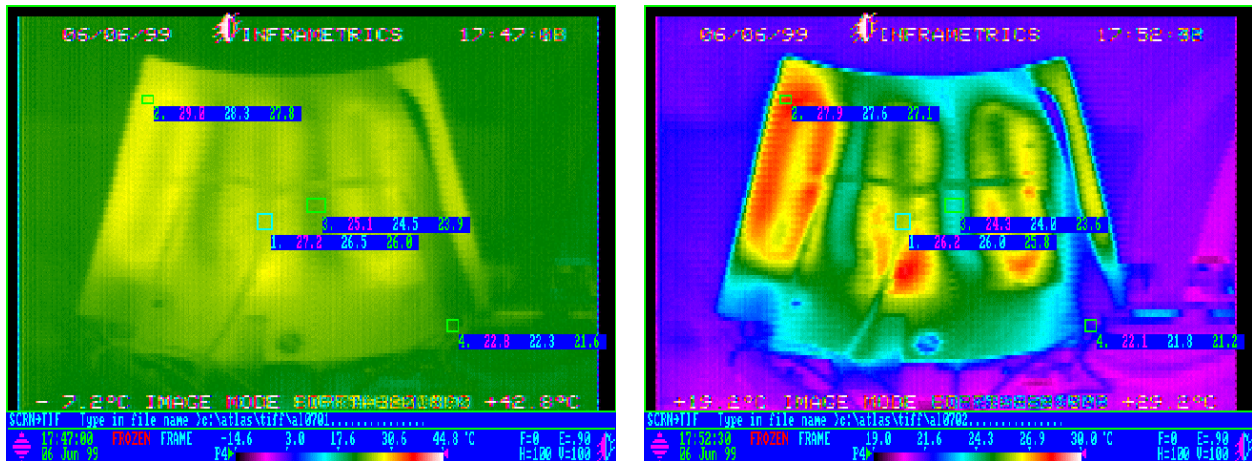


Figure 8. Thermal tests of aluminum tube prototype #7. Coolant is water at 21°C, 20 cc/sec. Power is 50W. Photo on left has scale for direct comparison with Figure 11 and photo on right has finer scale.

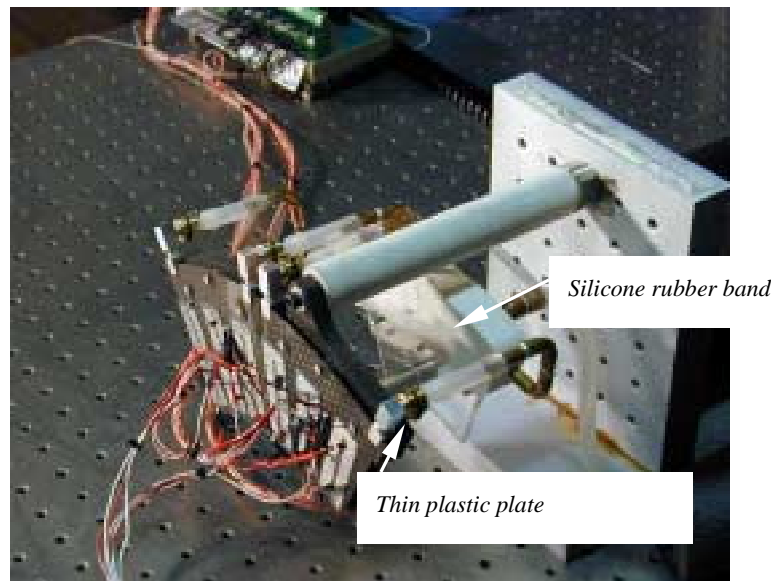


Figure 9. Close-up of the dual thermal structure test arrangement with partial view of coolant manifold.

For sector unit #4, the points of highest temperature increase above the inlet coolant temperature are located in the extreme lower corners of the facing overhang. See Figure 10 and Figure 11. In this location, heat must be conducted nominally 15mm before encountering a cooled zone. The overhang is like a fin being subjected to a constant heat flux. The thin facing material provides the primary path for heat conduction. Since the heat flux is constant in this region, the resulting temperature drop is very sensitive to the path length, an L^2 effect⁶. The 15mm distance is somewhat greater than anticipated due to the tube Triple U-pattern not matching the intended path exactly. Part of this problem is shrinkage caused by the tube carbonization cycle. HYTEC has plans to reconfigure the tube path for follow-on sector construction.

⁶ $\Delta T = \frac{qL^2}{2kt}$, where for ΔT , q is the heat flux, L the distance, k material conductivity, and t the material thickness.

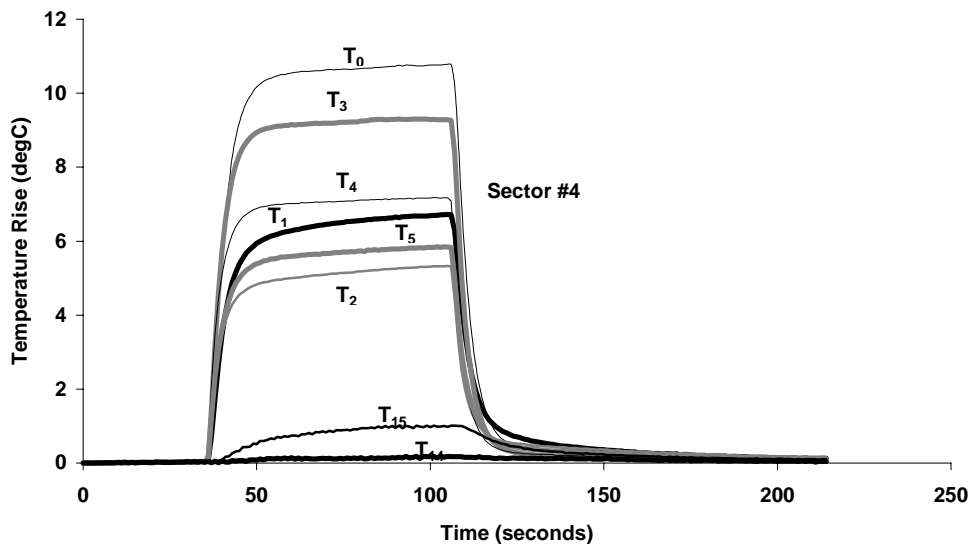


Figure 10. Thermal test results for unit #4, which is constructed with a carbon-carbon coolant tube with two layers of carbon fibers. Power input is 36W and coolant flow rate is 9 cc/sec with an inlet water temperature of 25°C. Peak temperature occurs at the outermost point of the facing overhang, both front and back facings, T_0 and T_3 . Temperatures T_2 , and T_5 are recordings on the body of the sector adjacent to the dummy heaters, whereas T_1 and T_4 are located on the heaters. T_{14} is on the inlet connection and T_{15} on the outlet connection.

Infrared images of sector #4 have been done at LBNL. See Figure 11. The temperature difference between surface recordings and the inlet bulk temperature are a linear function of power. This characteristic is consistent with expectations.

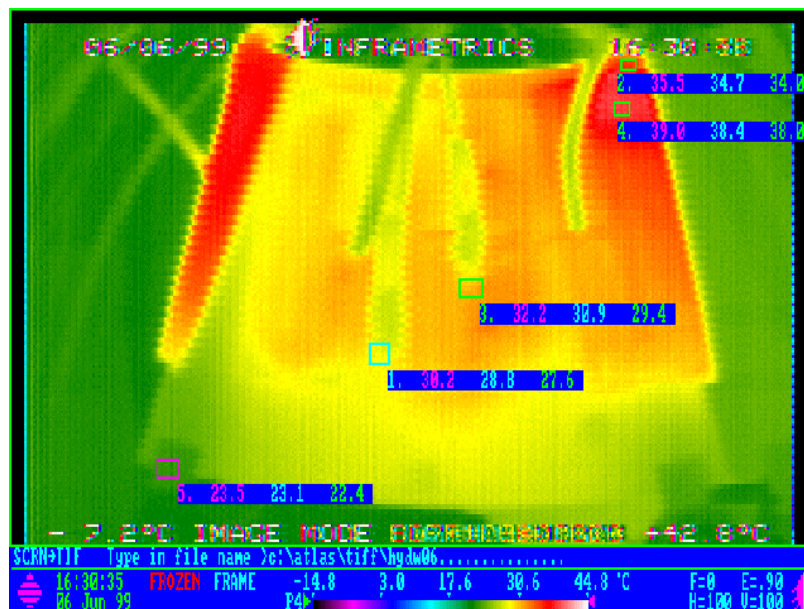


Figure 11. Thermal test of sealed-tube unit #4 at 20 cc/sec of room temperature water and 50W. The water enters on the left. Point 1 is between dummy heaters. Points 2 and 4 are on heaters. Point 5 is on the inlet connection and Point 2 on the edge of the faceplate. In all cases, the three values shown, from left to right, are highest, average and lowest pixels within the rectangle.

2.2.2.3 After Temperature Cycling

Temperature cycling measurements occur naturally as the thermal performance is measured although usually over a restricted range of temperature. Aluminum-tube prototype #4 was cycled between room temperature (22°C and -18°C) without heaters attached, the heaters attached and the thermal performance measured (also after the pressure cycling described in the next section). The thermal performance met the requirements. Prototype #3 was cycled between -15°C and 60°C four times. The temperatures measured on prototype #3 after this cycling at discrete points for low temperature operation are shown in Figure 12. Thermal measurements were repeated on this sector using liquid C₆F₁₄ coolant that resulted in temperature cycling multiple times from room temperature to about -20°C. No degradation in thermal performance has been observed after temperature cycling from room temperature to about -20°C for aluminum-tube prototypes measured so far. However, it should be noted that in all cases the dummy heaters were attached solely with CGL7018, which has a very, very low shear modulus and decouples any CTE mismatch between the silicon and the sector structure. Measurements are just starting on thermal cycling effects with dummy heaters attached both with CGL-7018 and with small tacks of UV epoxy that are required to prevent long-term creep using CGL-7018 alone. This will couple the silicon more rigidly to the faceplates, and will induce delaminating forces from the CTE mismatch between the silicon and the carbon-carbon. Measurements on aluminum-tube tests pieces after irradiation demonstrate that thermal performance can be met with silicon attached with CGL and UV tacks(see later). However, it remains to be proven that the full-sector design can withstand such forces, under all conditions. Tests are in progress on the sealed-tube sectors, but the intrinsic stability of these sectors is such that we expect no effects.

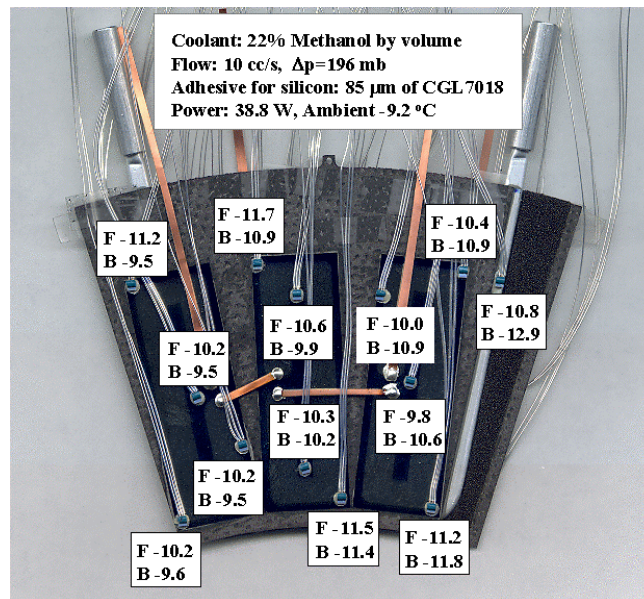


Figure 12. Typical results of measurements at low temperature, and after temperature cycling. Inlet fluid temperature was -15°C. F => front and B => back of sector.

2.2.2.4 After Pressure Cycling

The thermal performance after pressure cycling has been measured on aluminum-tube prototypes #4 and #6. Prototype #4 was cycled from atmospheric pressure to 5 bar absolute 24 times and then heaters attached. It was then cycled to 3.7 bar absolute 20 times with the heaters attached. The thermal performance of this prototype before and after cycling with heaters attached is shown in Figure 13 and Figure 14, respectively. The power was 60 W, the coolant was water at 11°C and the flow rate 20 cc/sec. No significant change in thermal performance was observed. Similar results were obtained with prototype #6, cycled to 5 bar absolute 140 times without heaters attached.

The thermal performance of sealed-tube sectors has been measured at discrete points after pressure cycling 150 times to 4 bar and after pressurizing to 10 bar. No degradation has been observed.



Figure 13. Aluminum-tube prototype #4 before pressure cycling (see text).



Figure 14. Aluminum-tube prototype #4 after pressure cycling (see text).

2.2.2.5 After Irradiation

The thermal performance of aluminum-tube prototype sector #3 was measured before and after irradiation with a Co^{60} source to 22 MRad. The before and after comparison is shown in Figure 15 and Figure 16, respectively. The power level was 36 W, the coolant was water at 23°C and the flow rate was 15 (after) and 17 (before) cc/sec. The temperature differential between the bulk coolant temperature and the silicon heater surface was the same within about 1°C, and even this small difference can be attributed to slightly different flow conditions. Thus there was no evidence of effects from radiation at 22 MRad.

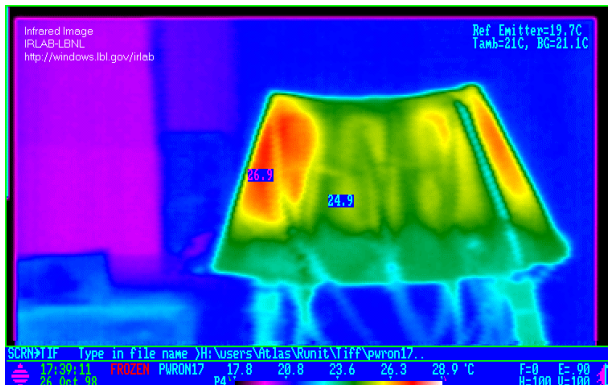


Figure 15. Before 22 MRad irradiation.

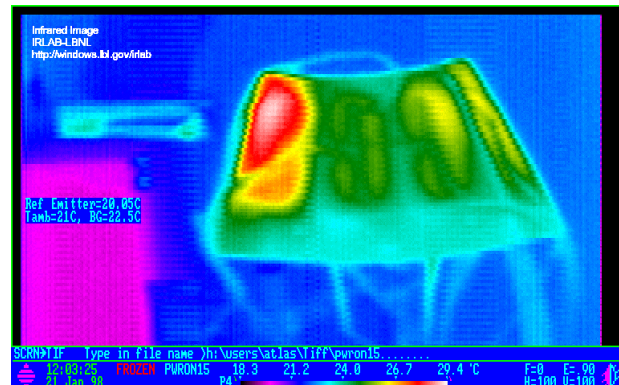


Figure 16. After 22 MRad irradiation.

An aluminum-tube test piece that is essentially one-third of a sector has been irradiated to 50 MRad. The dummy heaters were attached on both sides with CGL-7018 and UV epoxy tacks at the four corners. The thermal performance before and after irradiation is shown in Figure 17 and Figure 18, respectively. The thermal performance degrades by 1-2°C under the flow conditions used. The coolant was water/glycol at about 6°C but at a very low flow rate of about 2.5 cc/sec, which enhances the magnitude of any changes. This test piece was pressure cycled to 4 bar absolute 20 times and the thermal performance measured again. There was no appreciable change - see Figure 19 (note that the color scale is slightly different than in Figure 17 or Figure 18). The thermal performance was then measured after each of the following steps: temperature cycling to -30°C from room temperature; temperature cycling 20 times from room temperature to about 0°C; pressurization to 8 bar absolute; temperature increase to 100°C simulating loss of coolant (it took three minutes to reach 100°C after stopping the flow of coolant). No

appreciable change in thermal performance was seen after any of these steps. The thermal performance was then measured at a flow rate of 10 cc/sec with 5°C water/methanol(30%). The result is shown in Figure 20(the temperatures seen in the IR measurements around 5 degrees are 1-2°C lower than those obtained from discrete measurements). This test specimen easily meets thermal requirements after all normal, transient and fault conditions and after 50 Mrad. Inasmuch as its construction is identical to that of actual sectors, the aluminum-tube sectors should also meet thermal requirements under all conditions. Irradiation tests of sealed-tube sector test pieces are in progress.

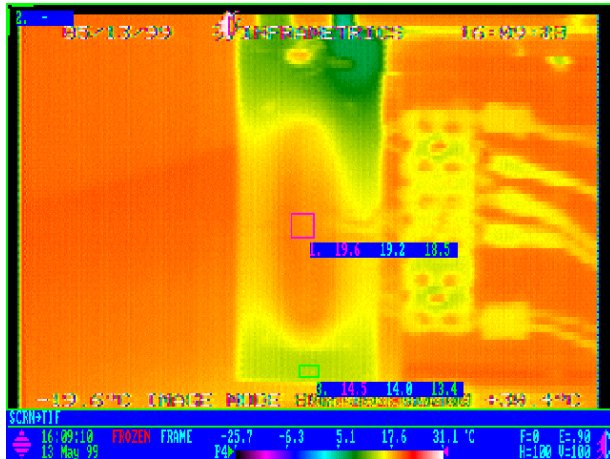


Figure 17. Test piece before irradiation.

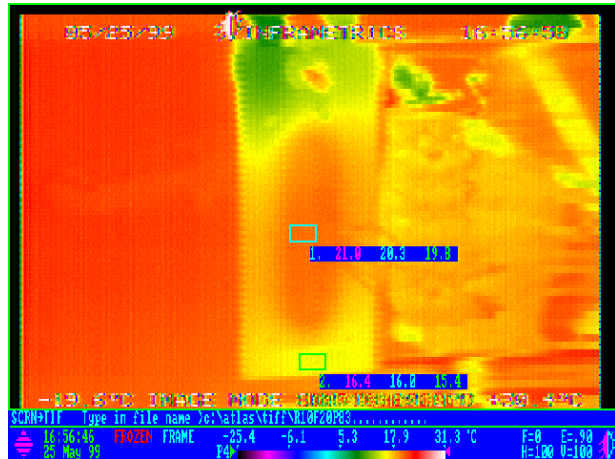


Figure 18. Test piece after 50Mrad irradiation.

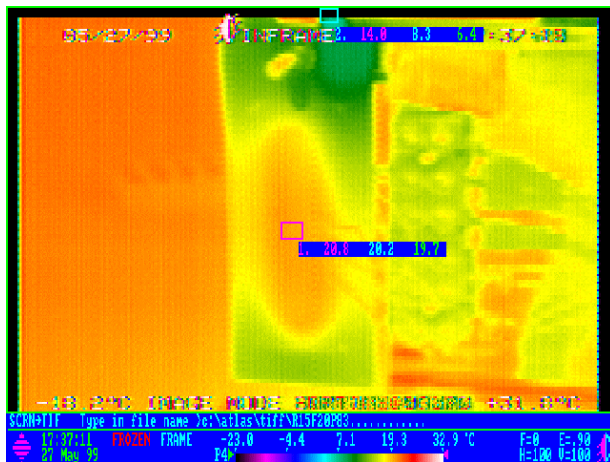


Figure 19. Test piece after 50 MRad and after pressure cycling to 4 bar absolute 20 times.

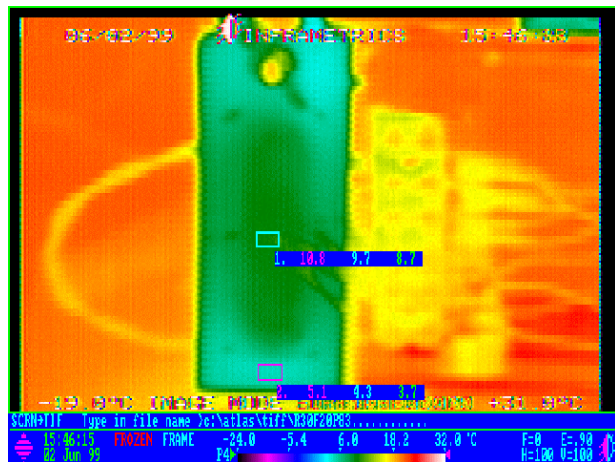


Figure 20. Test piece after all stress testing with 4°C water/methanol coolant at 10 cc/sec - see text.

2.2.2.6 After Transient and Fault Conditions

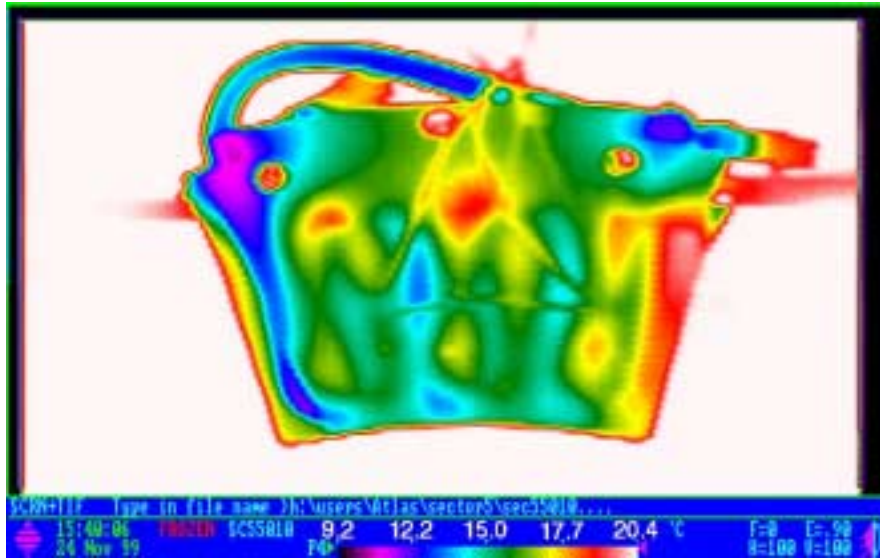


Figure 21. Aluminum-tube prototype #6 after pressure conditions described in the text.

Thermal measurements on aluminum-tube prototype #6 were made after cycling to 7 bar absolute without heaters attached. This followed the cycling to 5 bar absolute described previously. The thermal performance of this prototype met requirements, as can be seen in Figure 21. The power level was 50 W, the coolant was water/methanol at 11°C and the flow rate 10/cc/sec.

Measurements of complete aluminum-tube sectors have not yet been done at 8 bar absolute, the recently established single fault maximum pressure. A complete set of measurements to simulate no-flow conditions also have not yet been done. However, measurements on the irradiated test piece indicate that transient and fault condition requirements can be met.

Thermal measurements already shown for the sealed-tube sectors #4 were done after pressurizing to 10 bar absolute. A loss-of-coolant fault should have little effect on this design.

2.2.2.7 Measurements with Evaporative Cooling

Evaporative cooling measurements have been done with an ESLI prototype sector with C_4F_{10} but with a design configuration corresponding to an obsolete disk layout. A direct comparison to measurements using water/methanol was made. These measurements were made about one year ago. A good correlation was observed between the thermal performance using water/methanol at the exhaust temperature used in the C_4F_{10} measurements. An attempt was made to compare the measurements with calculations of the expected performance of C_4F_{10} evaporative cooling and extrapolate to the use of C_3F_8 evaporative cooling.⁹ These calculations indicated that a hydraulic diameter larger than 2.4 mm, which is the hydraulic diameter of aluminum-tube prototype #6, would be needed but there is considerable uncertainty in these extrapolations. It is planned to compare directly the thermal performance of aluminum-tube sectors (#7 and #8), which have hydraulic diameters of 2.4 mm with sectors (#9 and #10), which have hydraulic diameters of 3.3 mm, to fix finally the required hydraulic diameter required. The sealed-tube sectors have an hydraulic diameter of 3.2 mm, and one of these will be measured with C_3F_8 at the same time.

2.3 Stability Performance

2.3.1 Introduction

The stability performance of the disk sectors has been assessed by performing thermal cycling measurements and pressure cycling measurements. In each case the motion, primarily out-of-plane, of the sectors has been measured. This has been done using optical targets attached to the sectors and two types of optical coordinate measurement machines. Each of these optical CMMs has an accuracy of approximately 0.002 mm (rms) in the plane of the sector faceplate and about 0.005 mm (rms) in the out-of-plane (Z) measurements. More precise measurements of the Z motion has been done at HYTEC, Inc using TV Holography,

which has an intrinsic accuracy of about 0.00025 mm in the Z coordinate. The TV holographic technique has not been used so far for in-plane measurements but is being adapted for this purpose.

2.3.2 Test Samples and Single Sectors

Measurements have been done on a variety of single sectors and on a few test samples that simulate the sector construction techniques.

2.3.2.1 Thermal Effects

The out-of-plane deflection of aluminum-tube prototype #4 was measured by cooling the sector in cold box without coolant flow. Optical targets located on the sector were viewed by an optical CMM. A temperature change of 40°C (from 22°C to -18°C) resulted in out-of-plane motion of less than ± 0.020 mm relative to the location at room temperature. The in-plane motion is negligible for a single sector well supported by the three support points. Similar distortion measurements were performed on prototype #3 before and after irradiation, and the differences were within measurement errors. These measurements have been done with dummy heaters attached only with CGL-7018 or without heaters.

An evaluation was made of the thermal stability of the dual thermal structure arrangement of sealed-tube sectors. The objective of this test was to quantify the thermal stability of the sandwich structure and to assess the potential impact on the stability from the coolant manifold.

A stability sensitivity coefficient, $\mu\text{m}/^\circ\text{C}$, is determined through several steps. First, the change in shape is recorded from power off to power on. This step change effectively produces a thermal gradient throughout the structure. The temperature distribution causes a corresponding dimensional change, reflected by out-of-plane motions of the surface.

As a further step in this process, in a power off condition, the thermal structure temperature is decreased gradually by circulating coolant. At various temperature plateaus, the shape change is recorded. For this test the temperature gradient through the thermal structure thickness is nominally zero, only the structure temperature ideally changes uniformly. This test condition simulates cooling the structure from room temperature to -15°C, the initial setting before power to the pixel detector is turned on.

In the final step, power is turned on with the structure at -15°C. A total shape change from room temperature to a powered operating state is then recovered from a series of recordings.

An initial holography test of the dual thermal structure is complete. A test from power-off to power-on at 18W per sector was performed at room temperature. The shape change is shown in Figure 22. It is difficult to discern the 1mm gap between structures, since the fringes of one sector blends with the other. A fringe count (1 fringe $\sim 0.26 \mu\text{m}$) reveals a peak distortion of $1.3 \mu\text{m}$ in Sector #4 and $1.56 \mu\text{m}$ in Sector #3. The peak distortions occur in the lower corners of the facing overhangs. The sector facings, exclusive of overhangs distort somewhat less. These results extrapolated to a 50W condition, suggest the sectors would distort 3.6 and $4.3 \mu\text{m}$ respectively.

Sensitivity coefficients, based on the peak temperatures and peak displacements, for Sectors #3 and Sector #4 are $0.39\mu\text{m}/^\circ\text{C}$ and $0.26\mu\text{m}/^\circ\text{C}$ respectively. A rough extrapolation to a condition of cooling the sectors from room temperature to -15°C (no power) would suggest a shape change of $15.6\mu\text{m}$ and $10.4\mu\text{m}$ for Sectors #3 and #4 respectively. Further testing is planned to see to what extent these changes are additive.

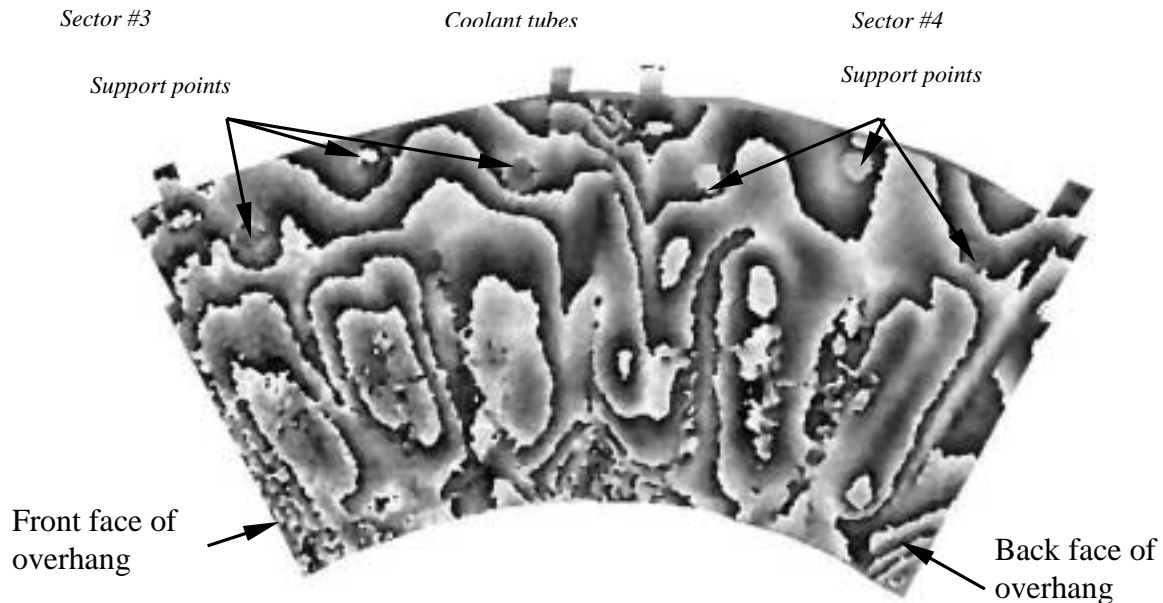


Figure 22. Phase map of fringe pattern illustrating out-of-plane distortions from power off to power on condition. Power state of 18W, with room temperature coolant at 9 cc/sec.

2.3.2.2 Pressure Effects

The distortions(out-of-plane) caused by pressure have been evaluated on aluminum-tube prototypes #4 and #6. Many points on prototype #6 were measured - see Figure 23. Data were taken up to about 5 bar absolute and after cycling 140 times to 5 bar absolute. The distortions in the "wing" regions on either side of the sector are the greatest. Distortions at the worst points are plotted in Figure 24. There is clear evidence of a permanent distortion (in the worst case about 40 microns). The magnitude of the distortion vs pressure is reduced after the initial distortion. The maximum distortion over most of the sector, not including the wing regions was less than 15 microns even at 7 bar absolute. Dummy heaters were mounted on this sector and the thermal performance easily met requirements, as already described above. The permanent distortions are attributable to distortions in the aluminum tube(confirmed by direct measurements of a bare tube). These results are (just) acceptable. Prototypes 7-10 have a thicker tube wall (0.029 mm rather than 0.020 mm) and will be tested, and should exhibit less distortion. Prototype #4 was tested to 5 bar absolute in a similar manner at -7°C and showed similar distortions.

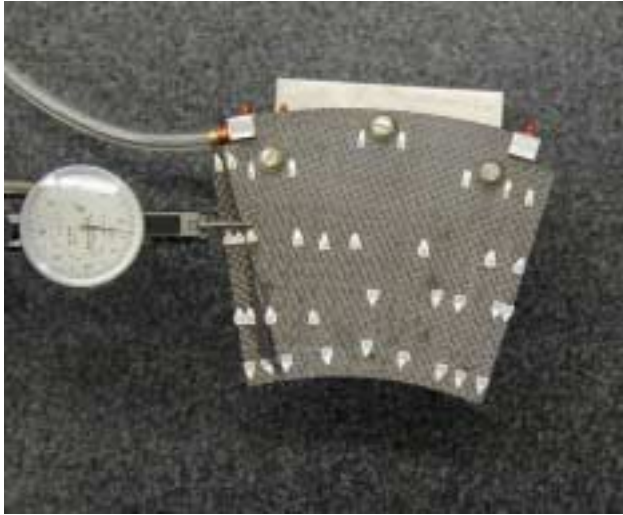


Figure 23. Prototype #6 showing points measured during pressure testing.

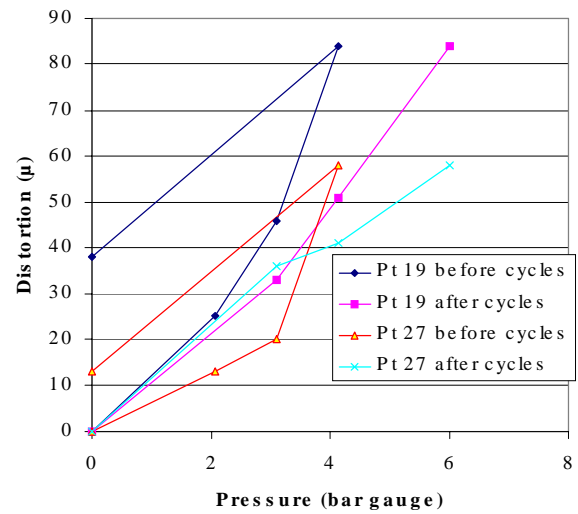


Figure 24. Distortion vs pressure at worst points before and after pressuring cycling(see text).

2.3.2.3 HYTEC Pressure Tests

Pressure tests were performed on HYTEC unit #4, using the setup shown in Figure 25. Stability is quantified by establishing the structure shape change with internal pressure using TV Holography.

The distortion observed for HYTEC unit #4 is quite low, 1.2 μm at 5 bar and 2.9 μm at 10 bar as shown in Figure 26. The low distortions are attributed to the high stiffness achieved by direct bonding of the carbon-carbon and the use of 0.5 mm thick faceplates.



Figure 25. Photograph of HYTEC sector pressure test setup. Inlet tube at upper right is open to pressure source. Exit tube at the left is sealed to prevent flow during the test.

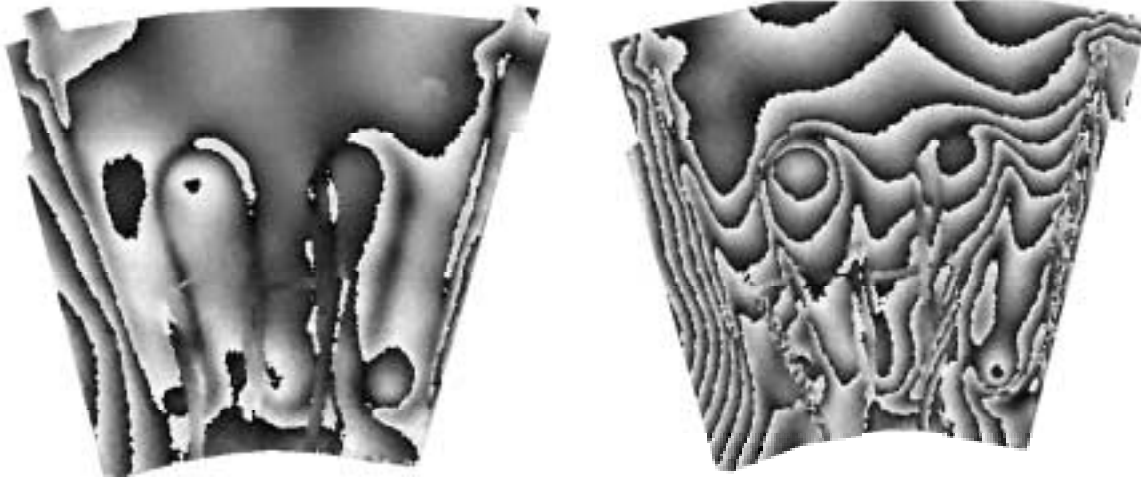


Figure 26. TVH results of pressure test with HYTEC unit #4. Left view illustrates fringe pattern for applied pressure differential of 5 bar. Right view illustrates pressure differential of 10 bar. Distortion from applied pressure amounts to 1.2 micron and 2.9 micron at 5 and 10 bar respectively.

2.3.2.4 Dynamic Stability

Some measurements of the dynamic response of prototype aluminum-tube sectors have been done using TV holography. The sector is firmly attached at the three support points and driven by a piezoelectric oscillator and the fringe pattern observed. This was done on prototype#3 before and after irradiation and the results are shown in Figure 27. The frequency response (of a single sector) is well above our nominal 100 Hz requirement. These measurements are in reasonable agreement with an FEA model.¹⁰

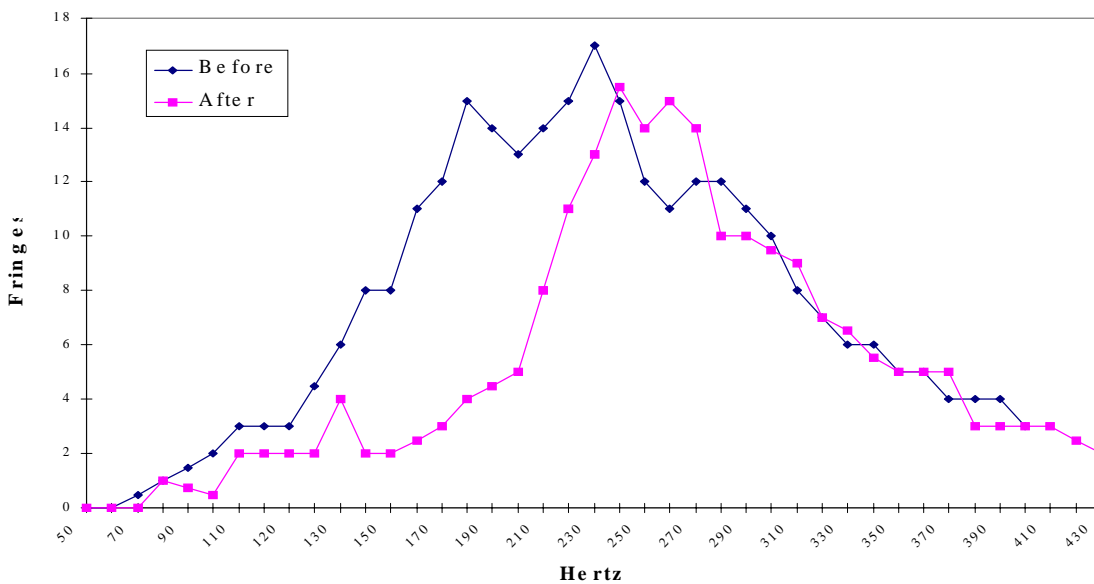


Figure 27. Frequency response of a prototype aluminum-tube sector before and after irradiation to 22 MRad.

2.3.2.5 Transient and Fault Conditions

Distortion measurements on aluminum-tube sectors after 7 bar absolute pressure have already been described. Similarly, we have already described measurements in sealed-tube sectors up to 10 bar. No distortion measurements have been made yet after a loss-of-coolant fault condition.

2.4 Prototype Disk

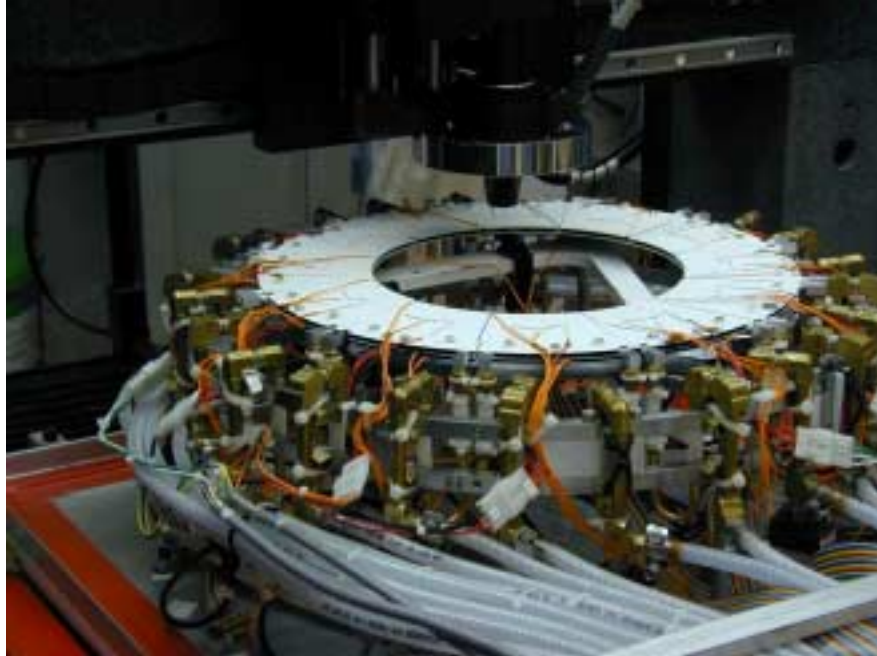


Figure 28. Prototype disk with 12 ESLI sectors in optical CMM. Cover of environmental box has been removed.

A complete disk of 12 sectors manufactured by ESLI was assembled and tested. Each sector had six dummy heaters. The sectors were attached to a prototype support ring designed by HYTEC, Inc and fabricated by Allcomp, Inc.¹¹ The disk-support ring was attached to an Invar support triangle at three points, which simulates the mounting expected in ATLAS. Coolant and power connections were made and the entire assembly placed in an environmental box on the table of an optical CMM as shown in Figure 28.

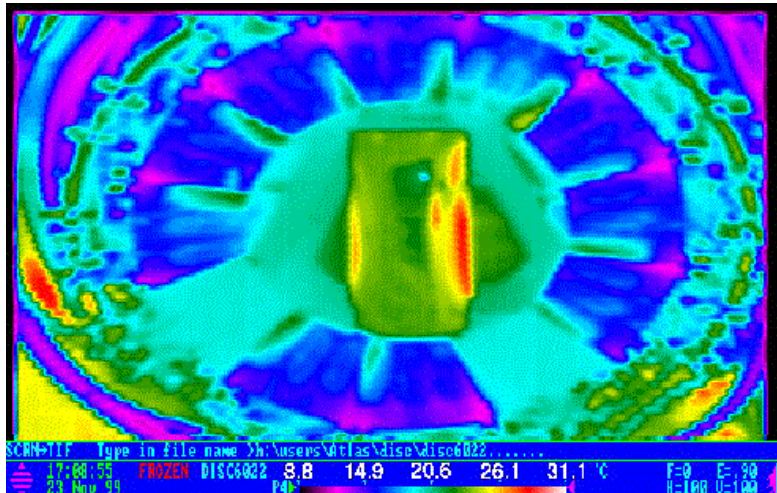
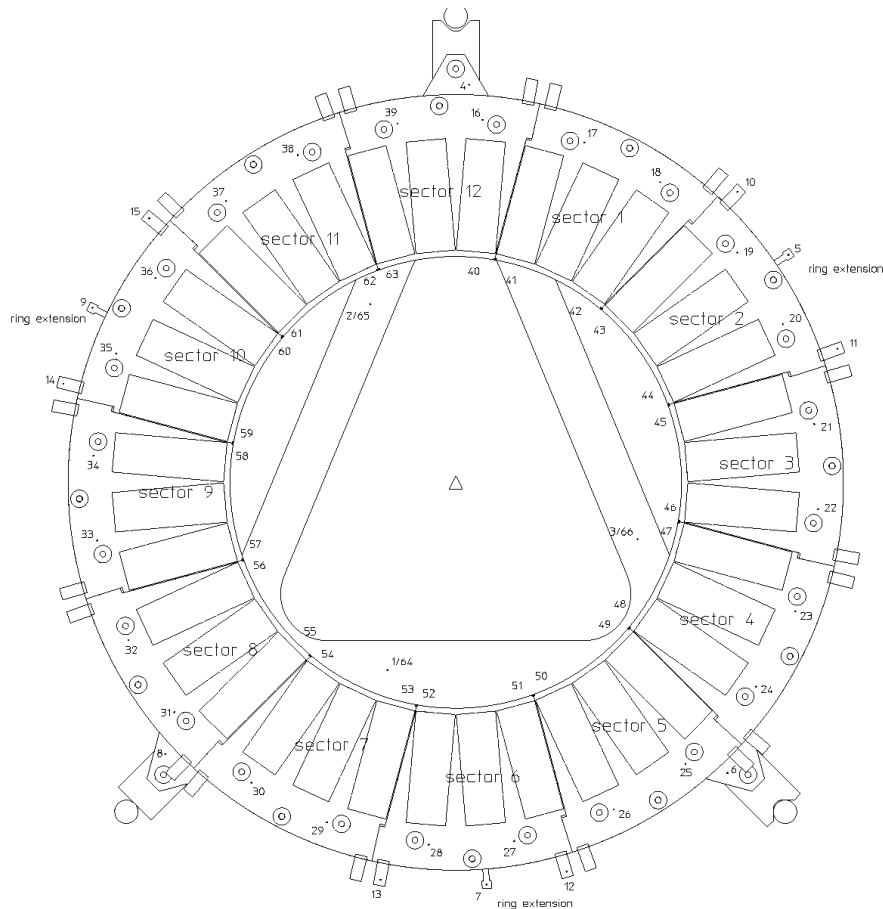


Figure 29. IR image of the disk prototype operated at 60W per sector. The inlet cooling temperature was 11°C. Two sectors were not powered(leaked).

Thermal measurements were made of the complete disk and are shown in Figure 29 for completeness. One sector has a "hot spot" reaching about 12°C (14°C) above the coolant temperature for 50(60)W of power.

Stability measurements were made by attaching optical targets to each sector (four locations), to the supporting ring and to the Invar support. The location of the targets is shown in Figure 30.



BACK of disk was mounted facing away from invar,
(toward viewer), sector numbers are clock positions as viewed.

Figure 30. Location of optical targets on prototype disk.

Temperatures and pressures on each sector were also recorded. The optical CMM was programmed to find and record the target locations.¹² Measurements were taken at different coolant temperatures down to -10°C . The distortions from temperature or pressure changes in the plane of the disk (X and Y) and out-of-plane (Z) were measured for each sector and for the ring. These extensive measurements are briefly summarized here.¹³

Distortions are determined by comparing the locations of the targets to an average base state taken at room temperature and no flow. A typical example of distortions observed at 60W per sector and at -10°C are summarized in Table 3. AVE is the average motion between the two states, SPREAD is the largest motion-smallest motion (including sign) and RMS is the standard deviation. The results are tabulated for different locations on the disk: on the ring, on a few coolant connections (in/out), at the outer radius of sectors (mount), the inner radius of sectors and the Invar support, which should not move. The largest distortions are in the Z (out-of-plane) motion but are well within requirements. In-plane motions are a few microns, also within the requirements. Although ESLI sectors are no longer considered for production, these measurements are indicative of the stability performance expected for a complete disk.

	<i>X</i>	<i>Y</i>	<i>Z</i>
<i>RMS (ring)</i>	0.0038	0.0055	0.0073
<i>RMS (in/out)</i>	0.0088	0.0052	0.0111
<i>RMS (sector @ mount)</i>	0.0023	0.0041	0.0083
<i>RMS (sector @ inner R)</i>	0.0028	0.0033	0.0091

<i>SPREAD (ring)</i>	0.0105	0.0134	0.0180
<i>SPREAD (in/out)</i>	0.0206	0.0133	0.0323
<i>SPREAD (sector @ mount)</i>	0.0079	0.0141	0.0320
<i>SPREAD (sector @ inner R)</i>	0.0107	0.0134	0.0378
<i>SPREAD (invar, final)</i>	0.0041	0.0018	0.0014

<i>AVE (ring)</i>	-0.0027	-0.0005	0.0014
<i>AVE (in/out)</i>	-0.0005	0.0014	0.0013
<i>AVE (sector @ mount)</i>	-0.0013	0.0002	0.0014
<i>AVE (sector @ inner R)</i>	-0.0010	-0.0012	0.0135
<i>AVE (invar, final)</i>	-0.0008	-0.0005	-0.0016

Table 3. Example of distortions measured at -10°C and 60W as explained in the text. Units are mm.

2.5 Material

The radiation length of a disk sector, averaged over the active region, is desired to be $\leq 0.7\% X_0$, assuming other requirements can be met. The radiation length of aluminum-tube prototype sector #6, based on measured weights, is summarized in Table 4. A number of fabrication options for aluminum-tube sectors remain and the potential impact of these on the radiation length, scaling from the measured weights of prototype #6, is given in Table 5.

	<i>RADIATION LENGTH(%)</i>
<i>Faceplates</i>	0.256
<i>Al tube</i>	0.162
<i>Foam</i>	0.031
<i>Hard points</i>	0.008
<i>CGL+glass beads</i>	0.047
<i>Cyanate ester</i>	0.035
<i>TOTAL</i>	0.539

Table 4. Radiation Length of Aluminum-tube Prototype Sector #6.

Faceplate Thickness	Tube Interior Dimensions	Tube Wall Thickness	Radiation Length(%)
300 microns	1.69mmx4.06mm	200 microns	0.539
432	1.69mmx4.06mm	200	0.652
300	1.69mmx4.06mm	290	0.610
432	1.69mmx4.06mm	290	0.723
300	2.743mmx4.191mm	200	0.572
432	2.743mmx4.191mm	200	0.685
300	2.743mmx4.191mm	290	0.658
432	2.743mmx4.191mm	290	0.771

Table 5. Radiation Length of Options for Aluminum Tube Sectors.

The radiation length of the sealed carbon-carbon tube sectors and possible means for material reduction are summarized in Table 6. Some attempt is being made to reduce the amount of adhesive. Improvements in this area will require special applicators and control. Consequence of lowering the mass too much is an increase in thermal impedance. Reduction in the faceplate thickness will reduce the stability, but the effect remains to be measured.

Element	Parameter	Actual weight(gm)	Radiation Length(%)
Face plates-CC	0.5 mm	12.48	0.383
Double Wall Carbon Tube	0.5 mm	4.6	0.217
Adhesive-AIT EG 7858	~0.1 mm	3.2	0.113
Hard points			0.008
Sum			0.721
Variations			
Face plates-CC	0.41	10.23	0.314
Single Wall Carbon Tube	0.25	2.25	0.106
Delta effect			-0.18
Realistic goal			0.6 to 0.65

Table 6. Radiation length of sealed tube sectors and possible means to reduce material.

2.6 Miscellaneous

Corrosion resulting from galvanic action between the aluminum tube and the carbon-carbon faceplates or foam is prevented by anodizing the aluminum tube and by using glass beads in the CGL-7018 to prevent direct contact between the tube and the faceplates.

Corrosion of the aluminum tubes resulting from the C_3F_8 has not yet been studied by the pixel group. Information from the manufacture indicates that corrosion of aluminum will not occur in the absence of water above the saturation point in the fluid.¹⁴ Since aluminum tubes are to be used throughout the pixel and SCT evaporative cooling system, a unified effort to investigate this point is underway.

Carbon-carbon is an electrical conductor. Dust or particles from the surface may be a problem in the presence of the bias voltage for the silicon sensors or other voltages. This can be prevented by properly impregnating the carbon-carbon faceplates, although there is a tradeoff in thermal performance through the resin (cyanate ester) and ensuring the absence of particles or dust. The foam is friable and must be sealed to ensure the absence of particles. This has not yet been done on any prototypes.

2.7 Interfaces

In this section we summarize briefly the ability of the disk sector designs to meet interface requirements.

2.7.1 Mounting to the Disk Support Ring

The location of sectors on the disk support ring is determined by precision pins located in the 0.125"(3.175 mm) holes in the sector and the mating holes in the disk ring. The sectors are held against the ring by using the pins in a bolt/nut combination. The prototypes that have been built so far rely on the precision of the holes in the ring and the sectors for absolute alignment. The sector design, precision holes, is frozen, but the exact configuration of the holes in the support ring remains open (simple holes, holes plus slots,...) and the material of the pins and bolts/nuts has not been finally determined. Options will be explored with the second prototype ring.

2.7.2 Coolant Connections

The cooling tube within a sector must be terminated to a coolant connection. This is done using a square-to-round transition piece as shown in Figure 31 for the aluminum-tube sector. A similar transition piece is used for the sealed-tube sector. These are glued to the sector cooling tubes. The current baseline adhesive (for aluminum tube sectors) is Hysol EA 9396, and some attachment of these pieces has also been done using 3-Aminopropyltriethoxysilane to enhance bonding. A temporary fitting¹⁵ is used for testing with liquid coolant as part of the sector QC procedure and after module attachment and pixel module testing. Permanent connections of exhaust or capillary tubing for evaporative cooling are planned to be glued connections using the same adhesive given above. A program is underway to validate the reliability of these connections with test pieces, like those shown in Figure 31, under pressure and temperature cycling and fault conditions.



Figure 31. Test piece showing square-to-round transition from sector cooling to other cooling connections.

2.7.3 Module Attachment

The tests of prototypes described above have been done using CGL-7018 with and without UV-curing epoxy tacks at the corner of the dummy silicon heaters. The baseline scheme for module attachment is to use about 0.050-0.075 mm of CGL-7018 that is screened into the sector (see Figure 32). The modules are then placed precisely and tacked into position firmly using tiny beads about 1x1 mm², of UV curing epoxy¹⁶, nominally at the four corners - see Figure 33. This technique has been used on some prototypes as already described above and appears, so far, to meet the requirements. However, additional tests of the robustness of the sector with dummy heaters attached is required and a final decision about where precisely to locate the UV tacks on real modules (on the electronics chips, to the sensor, both...) remains to be decided. Prototype tooling to attach modules to sectors is complete and trials are well underway. And a comprehensive test program to evaluate different low modulus, thermally-conducting adhesives other than CGL-7018 has been launched for both staves and sectors.

2.7.4 Electrical

No measurements have been done yet with electrically active modules mounted on local supports. In principle, the local supports may be isolated, if necessary, from the disk support ring by using e.g. PEEK button material. Direct connections to the carbon-carbon faceplates may be done using conducting epoxy and there is ample room available for making these connections, if they are found to be necessary.

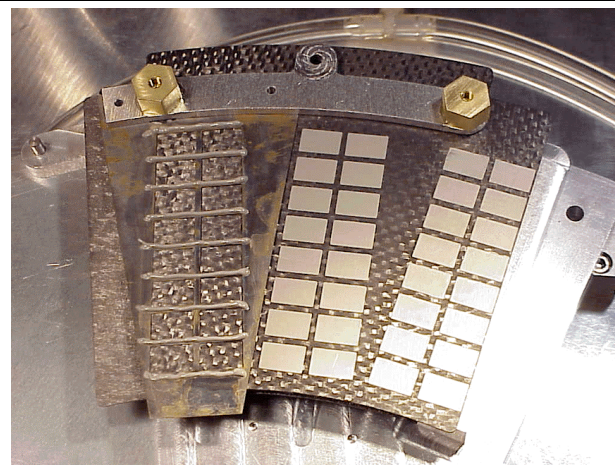


Figure 32. Example of screening CGL-7018 on to sector.

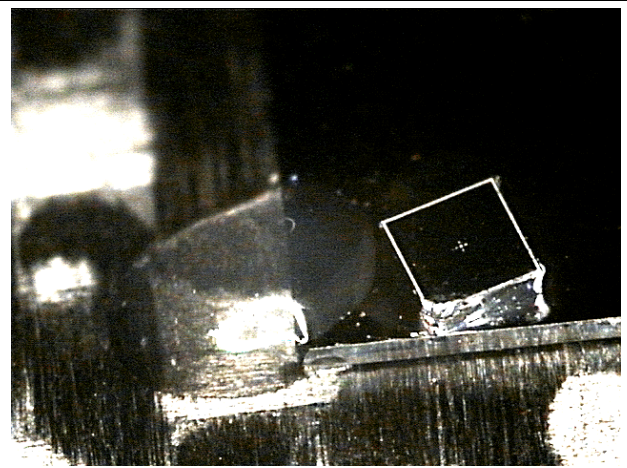


Figure 33. UV tack holding dummy silicon heater to sector faceplate. Survey target also shown is 1x1 mm²

2.8 Summary of Status and Critical Outstanding Issues

The current ability of the aluminum-tube and sealed-tube sectors to meet the requirements is summarized in Table 7.

Item	Requirement	Al-Tube	SealedTube
Normal Thermal Conditions			
ΔT from coolant to face of local support($^{\circ}C$)	≤ 12	≤ 10	$\leq 14^3$
Si temperature uniformity on local support($^{\circ}C$)	≤ 10	≤ 7	TBD
Meet all requirements after T cycles($\Delta T=20^{\circ}C$)	20 cycles	OK ¹	OK
Minimum temperature of silicon sensor	$-20^{\circ}C$	OK	OK
Normal Pressure Conditions			
Maximum normal operating pressure(bar absolute)	4.0	OK ¹	OK
Pressure cycling of ± 0.1 bar about 2 bar absolute	TBD cycles	TBD	TBD
Radiation Conditions			
Total dose	500,000 Gy (50,000,000 Rads)	OK ²	TBD
Material			
Radiation length(average over active area) - goal	≤ 0.7	≤ 0.77	≤ 0.72
Transient and Fault Conditions			
Minimum temperature on start-up of cooling	$-35^{\circ}C$	OK ²	TBD
Once-per-lifetime pressure fault for one hour	8 bar absolute	8 bar ²	10 bar
Once-per-lifetime temperature fault for 60 sec.	$50^{\circ}C$	OK ²	TBD
Miscellaneous Conditions			

<i>Conducting particles from carbon or other materials</i>	<i>Not allowed</i>	<i>TBD</i>	<i>TBD</i>
<i>Corrosion from all sources</i>	<i>Prevent</i>	<i>TBD</i>	<i>OK</i>
<i>Erosion from fluid flow</i>	<i>Prevent</i>	<i>TBD</i>	<i>TBD</i>
<i>Repair after complete assembly</i>	<i>Not required</i>	<i>OK</i>	<i>OK</i>
<i>Surface characteristics</i>	<i>Compatible with module attachment</i>	<i>OK</i>	<i>OK</i>
Envelopes and As-Built Tolerances			
<i>Faceplates as cut(mm)</i>	± 0.25	± 0.10	± 0.10
<i>Thickness of sector not including support buttons(mm)</i>	≤ 5.0	<i>OK</i>	<i>OK</i>
<i>Faceplate planarity(mm)</i>	± 0.075	<i>TBD</i>	<i>TBD</i>
Survey Tolerances			
<i>Reference targets on faceplates to mounting holes(mm)</i>	± 0.010	<i>OK</i>	<i>OK</i>
<i>Reference targets front-to-back sides(mm)</i>	± 0.025	<i>TBD</i>	<i>TBD</i>
Stability Tolerances			
<i>Z (out-of-plane)(mm)</i>	± 0.10	± 0.08	± 0.02
<i>Y(R) in-plane(mm)</i>	± 0.065	<i>OK</i>	<i>OK</i>
<i>X(ϕ) in-plane(mm)</i>	± 0.006	<i>OK</i>	<i>OK</i>

¹ Demonstrated for bare sectors without silicon tacked in place and for irradiated test piece.

² Demonstrated for irradiated test piece only.

³ Current status. A change in tube shape should reduce this enough to meet requirements.

Table 7. Summary of current ability of aluminum-tube and sealed-tube sectors to meet requirements.

There are many design issues remaining to be addressed but some are more critical than others. Measurements on more than one or two sectors are required for both design options - more statistics is required. In addition, a QC method to assess the thermal performance of the sectors before attaching modules has not been developed. Attaching temporary heaters, heating with IR lamps, and other methods will be tried but a firm procedure has not been established.

The most critical issues for the aluminum-tube sector are:

- Operation with the baseline coolant and selection of the tube inner dimensions (hydraulic diameter). This affects also the radiation length of the sector.
- Demonstration under all conditions, with sufficient statistics, of the reliability of the CGL-7018 thermal joint between the tube and the faceplate. In particular, measurements must be done with the silicon dummy heaters more rigidly attached with UV tack, which is the current plan, so that delaminating forces are properly imposed. Thermal performance appears to meet requirements from measurements, but stability performance remains to be assessed in detail.
- Demonstration that requirements, particularly thermal performance, can be met after pressure and temperature fault conditions for a complete sector.

The most critical issues for the sealed-tube sector are:

- Continued demonstration that sealed-tubes can be manufactured reliably to meet the pressure requirements and not leak
- Demonstration that the thermal performance can be met over a number of sectors.
- Feasibility of meeting requirements with thinner faceplates.
- Performance after irradiation.

3 Work Plan Summary

3.1 Introduction

The fabrication and test of additional sectors for both design options is in progress. The work program will focus first on addressing the critical issues outlined above but eventually all requirements. A key goal is to obtain information on more sectors - statistics - and to establish a thermal QC program for either sector design.

3.2 Sealed-tube Plan

A 2nd composite disk support ring designed by HYTEC is complete and will be used for testing a full complement of 12 sectors, in a disk configuration typical of the ATLAS Pixel Detector. See Figure 34 below. Thermal stability of both the individual ring and a complement of 12 sectors assembled onto the ring will be evaluated for temperature conditions simulating the detector application. In addition to these system tests, HYTEC intends to construct several sectors with 0.4 mm facings with the objective of reducing the amount of support material. These sectors will be subjected to the full standard evaluation tests, in a manner identical to that planned for the aluminum-tube sectors – see below. Sectors will be tested with evaporative C_4F_{10} at HYTEC and one or more sectors will be tested at CERN with evaporative C_3F_8 . Test pieces have been built and will be irradiated.

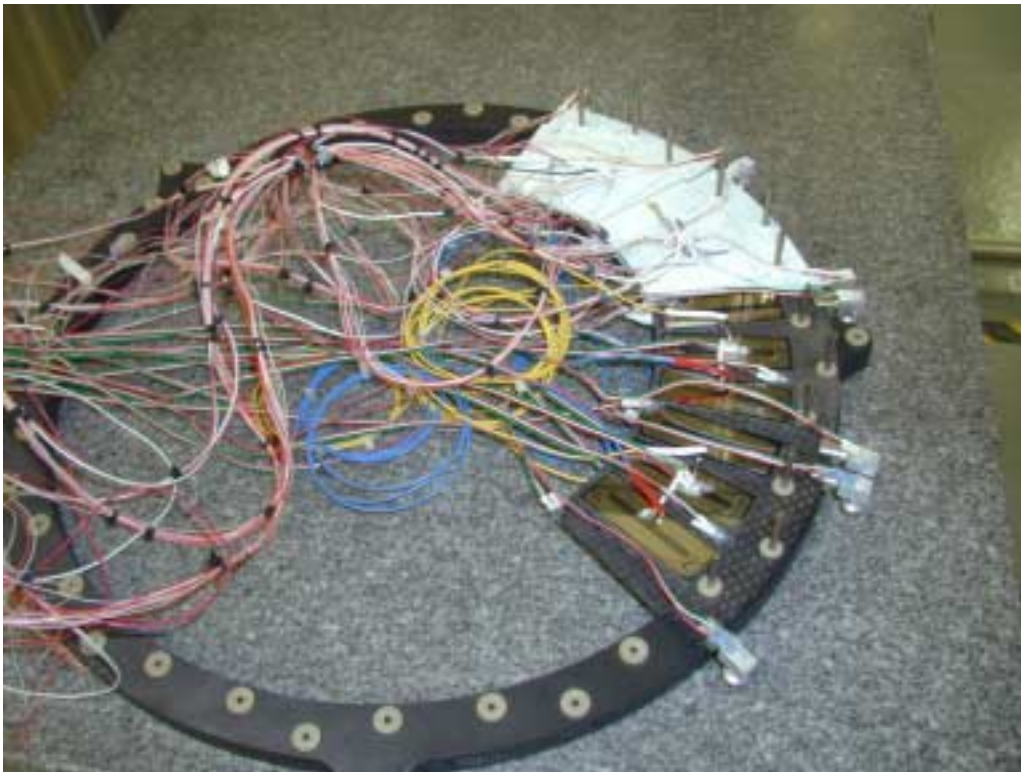


Figure 34. Second prototype disk using sealed-tube sectors under assembly at HYTEC, Inc.

3.3 Aluminium-tube Plan

Prototypes 7-10 are planned to be tested in June with evaporative C_3F_8 at CERN. These sectors differ in the hydraulic diameter of the tubes. They will be tested operating singly, in series and in parallel to determine the optimal hydraulic diameter and to compare with calculations of the cooling performance of the evaporative system.

These sectors and additional sectors (as well as sealed-tube sectors) and radiation test pieces will be subjected to a test protocol to verify that requirements can be met. Dummy silicon heaters will be attached with CGL-7018 only (or similar low modulus

materials) and with CLG-7018+UV-cured epoxy tacks(or just with a low modulus adhesive) to address the critical issue of delaminating forces introduced by the CTE mismatch between silicon and carbon-carbon. In brief this protocol is the following:

- Survey the sector before imposing significant thermal or pressure loads
- Cool with water/methanol at 10-15⁰C in air and establish a thermal base state with IR thermography
- Perform temperature cycling tests, determine distortions and resurvey and remeasure thermal performance
- Perform pressure cycling tests, determine distortions and resurvey and remeasure thermal performance
- Establish fault conditions and resurvey and remeasure thermal performance

A similar measurement protocol will be performed on additional test pieces irradiated to 50 MRad. It is also planned to build additional sectors with 300 micron thick faceplates to compare their stability performance to sectors with 425 micron thick faceplates.

¹ ATLAS Document No. ATL-IP-EM-0026 Pixel Local Supports Overview - Final Design Review.

² ATLAS Document No. ATL-IP-EP-0005, Pixel Local Support Requirements - Final Design Review.

³ ATLAS Document No. ATL-IP-FR-0001, ATLAS Disk Sector Fabrication and Specifications - Final Design Review

⁴ ATLAS Document No. ATL-IP-EP-0006, Local Supports Interfaces.

⁵ Energy Sciences Laboratory, Inc, 6888 Nancy Ridge Drive. San Diego, CA 92121-2232.

⁶ HYTEC, Inc, 110 Eastgate Dr., Los Alamos NM 87544.

⁷ HYTEC-TN-DOE/SBIR-04, January 2000.

⁸ Smaller test pieces for studies after irradiation were used because of size limitations of the Co⁶⁰ source that was used in the irradiation.

⁹ D. Bintinger, Lawrence Berkeley National Laboratory, "Evaporative Cooling Calculations", presentation at CERN, November 1999. See

http://edms.cern.ch/TWDM/fcgi/twdmdoc/ATL/Get/ROOT/_1000069889/_1799526688/_1904596489/_1814683311/1831898395/evap_cool_calcs_updated.pdf

¹⁰ HYTEC TN-1060200, "Thermoelastic Static and Modal Analysis of Composite Support Ring for the ATLAS Pixel Detector Planar Array", W. O. Miller, June 2000.

¹¹ Allcomp, Inc., 209 Puente Ave., City of Industry, CA, 91748.

¹² The measurement procedure may be seen at http://www-atlas.lbl.gov/mov/Proto_Disk_video.html.

¹³ A note on the measurement results may be found at http://www-physics.lbl.gov/~jtaylor/REPORT_comb.doc.

¹⁴ 3M Bulletin on Fluorochemicals in Thermal Management Applications.

¹⁵ FasTest connections - see <http://www.fastestinc.com>.

¹⁶ Norland Products, Inc., NEA123.